The impact of the transient uptake flux on bioaccumulation. Linear adsorption and first-order internalisation coupled with spherical semi-infinite mass transport.

Josep Galceran[†], Josep Monné[†], Jaume Puy[†] and Herman P. van Leeuwen[‡]

[†]*Departament de Química, Universitat de Lleida, Rovira Roure 191, 25198, Lleida, Spain*

[‡]*Laboratory of Physical Chemistry and Colloid Science, Wageningen University, Dreijenplein 6, 6703 HB Wageningen, The Netherlands*

corresponding author: galceran@quimica.udl.es

Abstract:

The uptake of a chemical species (such as an organic molecule or a toxic metal ion) by an organism is modelled considering linear pre-adsorption followed by a first-order internalisation. The active biosurface is supposed to be spherical or semi-spherical and the mass transport in the medium is diffusion-controlled. The analytical solutions for the transient flux and accumulated amounts can be used to discriminate between adsorption and internalisation parameters, which are inseparable in a steady-state flux interpretation. The concentration at the surface of the organism and the (intracellular) uptake flux pass through a maximum before coming to their steady-state values. For any combination of the parameters, the time necessary to reach a diffusive flux which differs by less than 10% from the eventual steady-state value can be directly read from a contour plot. For small micro-organisms, steady state is usually achieved in a short time and so the usual analysis based on the steady-state flux is a good approximation (except for combinations of large radii, low diffusion coefficients, important adsorption and slow internalisation kinetics). However, interpretation of the cumulative uptake requires (explicit or implicit) consideration of the large transient fluxes arising at short times. By considering an instantaneous steady state approximation, the linear regression of accumulation data outside the transient regime, i.e. at larger measuring times, allows for the discrimination between adsorption and kinetic parameters for small organisms as shown with literature data of lead uptake by *Chlorella vulgaris*.

keywords: uptake, bioaccumulation, mathematical model, transient, Chlorella

Introduction

Much experimental work in biouptake of either pollutants or nutrients by micro-organisms has relied on the interpretation of the data in terms of steady-state theories (Whitfield and Turner 1979;Morel and Hering 1993;Tessier et al. 1994;Stumm and Morgan 1996) in which the kinetics considered did not result in a time-dependent response function. However, the validity of the steady-state condition for the data has not always been explicitly checked, nor has it ever been derived from a rigorous mathematical framework. Thus, it seems timely to critically analyse the range of validity of the steady-state option by developing a comprehensive transient model –even if it is a simple first approximation to a very complex problem.

A transient model is clearly needed if the uptake flux exhibits a certain evolution in time. Generally, with short-time uptake experiments becoming increasingly relevant and accessible (Hudson and Morel 1990;Knauer et al. 1997;Phinney and Bruland 1997;Croot et al. 1999;Kujawinski et al. 2000;Fortin and Campbell 2001;Slaveykova and Wilkinson 2002;Campbell et al. 2002), consideration of the transient flux will become more and more topical, especially for the interpretation of experimental plots where the cumulative uptake is not just a straight line through the origin. Moreover, analysis of the transient data provides a means to discriminate between adsorption and internalisation processes. Likewise, the distinction between influx and efflux and more detailed analysis of the internalisation mechanism require rigorous interpretation of initial fluxes. Knowledge of transient behaviour is also necessary to understand the characteristic relaxation times of the biosystem, i.e. the time needed to reach a new steady state after some perturbation such as the change of the activity of the bioactive species in the medium.

The model we develop here considers the three usual steps: diffusion, adsorption and internalisation (Whitfield and Turner 1979;Campbell 1995;Pinheiro and van Leeuwen 2001;Slaveykova and Wilkinson 2002). Dynamics are not only involved with the internalisation step, but also with the diffusion step, which is assumed to be negligible in the Free Ion Activity Model (Morel and Hering 1993;Tessier et al. 1994;Campbell 1995;Hudson 1998). For a dilute dispersion of sufficiently small organisms, with dimensions below some 10^{-4}m (Lazier and Mann 1989;KarpBoss et al. 1996), mass transport is adequately described by semi-infinite diffusion. Regarding adsorption, the linear regime (Henry isotherm) allows the derivation of analytical expressions for concentrations and fluxes (Holub 1966). The linear adsorption approximation can be also valid for a set of different isotherms applied to different sites –even if adsorption is not followed by internalisation at some of them-, provided they all are at low coverage in the linear regime. The treatment in this work is especially focused on fluxes, as they convey the vital information regarding the rate of accumulation of the bioactive species.

Mathematica code to compute expressions in this work is available free of charge via the Internet at http://www.udl.es/usuaris/q4088428.

1.- Modelling the biouptake.

1.1.- Formulation of the linear model

Consider the uptake of a given chemical species, which could be a metal ion, an organic molecule, etc., that will be referred to as M. This species M is present in the bulk of the medium at a concentration c_{M}^{*} and we assume that the only relevant mode of transport from the medium to the organism is diffusion. The internalisation sites are taken to be located on the spherical surface of the micro-organism or on a semi-spherical active

surface domain, with radius r_0 (see Fig. 1). Thus, mass conservation in time prescribes the diffusion equation:

$$\frac{\partial c_{\mathrm{M}}(r,t)}{\partial t} = D_{\mathrm{M}}\left(\frac{\partial^2 c_{\mathrm{M}}(r,t)}{\partial r^2} + \frac{2}{r}\frac{\partial c_{\mathrm{M}}(r,t)}{\partial r}\right) \quad (1)$$

M is adsorbed onto the surface by a process that is assumed to be fast enough (when compared with the diffusion and the internalisation processes) to ascertain local equilibrium (so, kinetically controlled cases (Morel and Hering 1993;Hudson and Morel 1993;Hudson 1998) are not analysed here). We consider the case of a linear adsorption isotherm, i.e. a linear relationship between the surface concentration (Γ_{M} units of mol m^{-2}) and the medium volume concentration of M just outside the adsorbed layer at the organism surface $c_{\mathrm{M}}(r_0,t)$:

$$\Gamma_{\mathrm{M}}(t) = K_{\mathrm{H}}\, c_{\mathrm{M}}(r_0,t) \quad (2)$$

where K_{H} stands for the linear (Henry) adsorption constant. This hypothesis is more realistic the lower the concentration of M, as in the case of trace species. For larger concentrations of M (in comparison with the number of adsorption sites), other isotherms accounting for saturation effects should be used.

Once adsorbed, we assume that M is internalised following a first-order kinetics process with internalisation rate constant k (Morel and Hering 1993;van Leeuwen and Pinheiro 2001). Thus, the boundary condition arising from the conservation of mass (of M) at $r=r_0$ can be written as:

$$\frac{d\Gamma_{\mathrm{M}}(t)}{dt} = K_{\mathrm{H}}\frac{dc_{\mathrm{M}}(r_0,t)}{dt} = D_{\mathrm{M}}\left(\frac{\partial c_{\mathrm{M}}(r,t)}{\partial r}\right)_{r=r_0} - k\, K_{\mathrm{H}} c_{\mathrm{M}}(r_0,t) \quad (3)$$

where k (given in s^{-1}) is assumed to be independent of the surface concentration Γ_M. The remaining boundary conditions for the mass transport process are a fixed bulk concentration at large distance from the surface

$$c_M(r,t) = c_M^* \qquad r \to \infty \qquad t \geq 0 \tag{4}$$

and an initially homogeneous distribution of M in the medium:

$$c_M(r,t) = c_M^* \qquad r \geq r_0 \qquad t = 0 \tag{5}$$

Note that condition (4) implicitly assumes that depletion of the bulk medium is negligible and that diffusion layers of different active biosurfaces do not overlap (Wolf-Gladrow et al. 1999).

Apart from the concentration at the surface $c_M(r_0,t)$, relevant quantities to characterise the system are the incoming diffusional mass transport flux at the surface

$$J_m(t) \equiv D_M \left(\frac{\partial c_M(r,t)}{\partial r} \right)_{r=r_0} \tag{6}$$

and the uptake (or internalisation) flux

$$J_u(t) \equiv k\,\Gamma_M(t) = k\,K_H\,c_M(r_0,t) \tag{7}$$

Note that, for simplicity, a positive sign is assigned to fluxes towards the surface.

The cumulative internalised amount (Kuma et al. 2000) is given by the time integral of the uptake flux

$$\Phi_u(t) \equiv \int_0^t J_u(t)\,dt \tag{8}$$

representing the amount of matter that has been internalised per unit of surface area, so that $4\pi r_0^2\,\Phi_u$ yields the amount taken up per (spherical) cell from the beginning of the process.

On the other hand the total cumulative supply to the biosurface Φ_m can be defined as

$$\Phi_m(t) \equiv \int_0^t J_m(t)\,dt \tag{9}$$

With minor changes, the formulation given so far can be extended to the case where M in the medium is associated with some ligand in a fully labile bioinactive complex (van Leeuwen and Pinheiro 2001). In this case, an additional simplifying condition would be that the amount of ligand is in such an excess that the concentration of M and complex are related linearly. In this excess ligand situation the effective diffusion coefficient is just a weighted average of the diffusion coefficients of the labile bioinactive complex and the free bioactive M (Heyrovsky and Kuta 1966;DeJong and van Leeuwen 1987).

1.2.- At low concentrations, adsorption followed by internalisation in any number of sites can be described with just two parameters

We highlight that the linear model presented in the previous section including just two parameters: K_H for the adsorption process and k for the internalisation kinetics is rigorous for any number of different (adsorption and internalisation) sites, as long as each one of them is described by a Henry isotherm (probably because of the low M concentration) followed by first-order kinetics and all adsorption processes are at equilibrium. For instance, the distinction between 2 types of sites: one physiologically active (which we label here with a subscript 1) and another non-active (labelled with subscript 2) type of sites is widely used (Bates et al. 1982;van Leeuwen and Pinheiro 2001;Slaveykova and Wilkinson 2002). Assuming Langmuirian isotherms for the 2-type-of-sites model one can write :

$$\frac{\Gamma_1(t)}{\Gamma_{\max,1}} = \frac{c_M(r_0,t)}{K_{M,1} + c_M(r_0,t)} \quad ; \quad \frac{\Gamma_2(t)}{\Gamma_{\max,2}} = \frac{c_M(r_0,t)}{K_{M,2} + c_M(r_0,t)} \tag{10}$$

where Γ_1 and Γ_2 stand for the surface concentration associated with sites of type 1 and 2 respectively (with $\Gamma_{\max,1}$ and $\Gamma_{\max,2}$ as their maximum values) and $K_{M,1}$ and $K_{M,2}$ are the half-saturation constants for each isotherm (equal to the inverse of the usual Langmuirian adsorption constant)(Morel and Hering 1993). According to this 2-types-of-sites approach, M is internalised only in sites of type 1:

$$J_u(t) = k_1 \Gamma_{\max,1} \frac{c_M(r_0,t)}{K_{M,1} + c_M(r_0,t)} \tag{11}$$

When $c_M(r_0,t) << K_{M,1}$ and $c_M(r_0,t) << K_{M,2}$, all the sites follow linear isotherms and comparison of eqn. (10) with (2) and (11) with (7) leads to the following equivalencies:

$$K_H = \frac{\Gamma_{\max,1}}{K_{M,1}} + \frac{\Gamma_{\max,2}}{K_{M,2}} \tag{12}$$

and

$$k = \frac{k_1 \Gamma_{\max,1} K_{M,2}}{\Gamma_{\max,1} K_{M,2} + \Gamma_{\max,2} K_{M,1}} \tag{13}$$

between these models.

In conclusion, K_H and k can be seen as global effective parameters averaging (with the appropriate weight) all the adsorption and internalisation characteristics of the different sites available on the surface when the concentration of M is low enough. The average nature of K_H and k renders them specially robust against changes such as the number of different types of sites considered.

2.- Expressions for fluxes and accumulated amount

2.1 Analytical solution for steady state

The solution for the steady-state concentration at the spherical surface c_M^{SS} (for simplicity we omit the spatial reference r_0) follows from eqn. (3) for $dc_M / dt = 0$

$$\frac{c_{\mathrm{M}}^{\mathrm{SS}}}{c_{\mathrm{M}}^{*}} = \frac{1}{1 + k\,K_{\mathrm{H}} r_0 / D_{\mathrm{M}}} \tag{14}$$

from which the steady-state diffusion flux at the surface can be computed as (Hudson 1998;Sanford and Crawford 2000)

$$J_m^{\mathrm{SS}} / c_{\mathrm{M}}^{*} = D_{\mathrm{M}} /(r_0 + D_{\mathrm{M}} / (k\,K_{\mathrm{H}})) = \left(r_0 / D_{\mathrm{M}} + 1/(k\,K_{\mathrm{H}})\right)^{-1} \tag{15}$$

Taking the inverse of each side of this expression leads to the interpretation of the "total uptake resistance" or "inverse of permeability" $c_{\mathrm{M}}^{*} / J_m^{\mathrm{SS}}$ being the sum of the "diffusional transport resistance" r_0 / D_{M} and the "adsorption-internalisation resistance" or "surface resistance" $1/(k\,K_{\mathrm{H}})$ (Oldham and Myland 1994;Hudson 1998). Decreasing the radius well below $D_{\mathrm{M}}/(k\,K_{\mathrm{H}})$ has a vanishing effect on the steady-state flux J_m^{SS}, as the limiting step is no longer diffusion-controlled but governed by the heterogeneous processes (adsorption+internalisation). On the other hand, if the couple adsorption + internalisation is much more effective than diffusion ($k\,K_{\mathrm{H}} >> D_{\mathrm{M}}/r_0$), then $c_{\mathrm{M}}^{\mathrm{SS}} \rightarrow 0$ and the limiting steady-state flux J_m^{*} for a spherical organism is recovered:

$$J_m^{*} = D_{\mathrm{M}} c_{\mathrm{M}}^{*} / r_0 \tag{16}$$

2.2 Analytical solutions for the transient flux and concentration at the surface

Existing solutions from the literature (Holub 1966;Holub and van Leeuwen 1984) can be expressed in terms of the auxiliary parameters

$$\alpha \equiv \frac{\sqrt{D_{\mathrm{M}} r_0} + \sqrt{D_{\mathrm{M}} r_0 - 4\left(D_{\mathrm{M}} K_{\mathrm{H}} + k K_{\mathrm{H}}^2 r_0\right)}}{2 K_{\mathrm{H}} \sqrt{r_0}} \tag{17}$$

and

$$\beta \equiv \frac{\sqrt{D_{\mathrm{M}} r_0} - \sqrt{D_{\mathrm{M}} r_0 - 4\left(D_{\mathrm{M}} K_{\mathrm{H}} + k K_{\mathrm{H}}^2 r_0\right)}}{2 K_{\mathrm{H}} \sqrt{r_0}} \tag{18}$$

The expression for the concentration at the surface $c_M(r_0,t)$ can then be formulated as

$$\frac{c_M(r_0,t)}{c_M^*} = \frac{c_M^{SS}}{c_M^*} + \frac{\beta\left(D_M - \alpha r_0\sqrt{D_M}\right)\mathrm{F}\left(\alpha\sqrt{t}\right) + \alpha\left(\beta r_0\sqrt{D_M} - D_M\right)\mathrm{F}\left(\beta\sqrt{t}\right)}{\alpha\beta(\alpha-\beta)K_H r_0} \tag{19}$$

where

$$\mathrm{F}(x) \equiv \exp(x^2)\,\mathrm{erfc}(x) \tag{20}$$

Exact analytical expressions are also available for the specific case where $\alpha=\beta$.

From the equation for the concentration, the expression for the flux is derived in a straightforward manner by applying the boundary condition (3) and the definitions (6) and (7). The result is

$$\begin{aligned}\frac{J_m}{D_M c_M^*} = \frac{J_m^{SS}}{D_M c_M^*} + \frac{1}{\sqrt{\pi D_M t}} + \\ + \left(\frac{2\sqrt{D_M}}{r_0} - \frac{D_M}{r_0^2\alpha} - \alpha\right)\frac{\mathrm{F}\left(\alpha\sqrt{t}\right)}{K_H(\alpha-\beta)} \\ - \left(\frac{2\sqrt{D_M}}{r_0} - \frac{D_M}{r_0^2\beta} - \beta\right)\frac{\mathrm{F}\left(\beta\sqrt{t}\right)}{K_H(\alpha-\beta)}\end{aligned} \tag{21}$$

By using an asymptotic expansion of F (Abramowitz and Stegun 1986), it can be shown that the concentration at the surface, and consequently the uptake flux J_u, goes through a maximum. For instance, in the curve for k=10^{-1} s^{-1} in Fig 2, $c_M(r_0,t)/c_M^*$ attains a maximum value of around 0.0068 at approximately t=21 s, overshooting the eventual steady-state value close to 0.005 given by eqn. (14).

The physical reason for the maximum in the time evolution of the concentration at the surface can be understood from the combination of the diffusion, adsorption and internalisation processes. In the limit of only adsorption (i.e. if internalisation were

absent: k=0), the $c_M(r_0,t)$ value would drop to 0 at t=0 and *increase* towards c_M^* without any maximum. In the limit of only internalisation (i.e. if adsorption were absent: K_H=0), the $c_M(r_0,t)$ value would *decrease* from the initial c_M^*-value to the steady-state value where internalisation is exactly compensated by diffusion. For the combined processes, adsorption prevails at shorter times (due to its equilibrium condition) and $c_M(r_0,t)$ increases up to a point where the corresponding J_u cannot be maintained by the diffusional flux J_m (which continuously decreases with t due to the depletion of M close to the surface). In fact, when J_u=J_m, the boundary condition (3) prescribes $dc_M(r_0,t)/dt = 0$, which is the condition for the maximum. Then, $c_M(r_0,t)$ begins to decrease towards c_M^{SS} because J_u>J_m. Such a type of transient overshoot phenomenon is not unusual: it has also been predicted for adsorption-internalisation in planar geometry (Holub and Koryta 1965) and in electrodic conversion of the reactant affected by a slow preceding chemical reaction (DeJong and van Leeuwen 1987). There are reported overshoots in short time biouptake experiments, such as Fig 1 in Knauer et al. (1997); Fig 6 in Sunda and Huntsman (1998); Fig 2 in Mirimanoff and Wilkinson (2000); Fig 8 in Campbell et al. (2002), although they could be due to a combination of various phenomena.

The practical relevance of the existence of the maximum depends on the corresponding concentration being sufficiently different from the final steady-state value. For instance, in the most peaked curve (k=1 s^{-1}) in Fig 2 the maximum concentration is 2.5 times c_M^{SS}, while for the curve with k=2×10^{-2} s^{-1} the maximum is just *one eighth* above the steady-state value. Thus, the maximum can be easily missed in cases with a low difference between the maximum and steady-state concentrations or with inadequate time spans.

2.3 Analytical Solutions for the cumulative uptake

Using the previous result (19) with (7) and (8), one finds

$$\begin{aligned}\Phi_u(t) = &-\frac{c_{\mathrm{M}}^* D_{\mathrm{M}} K_H^2 k\, r_0 \left(D_{\mathrm{M}} + k\, r_0 \left(K_H + r_0\right)\right)}{\left(D_{\mathrm{M}} + K_{\mathrm{H}} k\, r_0\right)^3} + J_m^{\mathrm{SS}}\, t + \frac{2 r_0^2 \left(J_m^{\mathrm{SS}}\right)^2}{c_{\mathrm{M}}^* D_{\mathrm{M}}^{3/2} \sqrt{\pi}} \sqrt{t} \\ &- \frac{c_{\mathrm{M}}^* k \sqrt{D_{\mathrm{M}}} \left(\alpha r_0 - \sqrt{D_{\mathrm{M}}}\right)}{\alpha^3 (\alpha - \beta) r_0} \mathrm{F}\left(\alpha\sqrt{t}\right) + \frac{c_{\mathrm{M}}^* k \sqrt{D_{\mathrm{M}}} \left(\beta r_0 - \sqrt{D_{\mathrm{M}}}\right)}{\beta^3 (\alpha - \beta) r_0} \mathrm{F}\left(\beta\sqrt{t}\right)\end{aligned} \tag{22}$$

Φ_m can be computed either integrating (21) or from the sum of the internalised amount and the adsorbed amount

$$\Phi_m(t) = \Phi_u(t) + K_{\mathrm{H}}\, c_{\mathrm{M}}(r_0, t) \tag{23}$$

which can be computed with expressions (19) and (22).

Notice that Φ_u vs. time will display an inflexion point when J_{u} has its maximum, swapping from an initially concave shape to a convex one.

3.- Evolution of flux and cumulative uptake

3.1 The impact of the radius

Fig. 3 plots the evolution of the fluxes J_m and J_u with time. As expected, the diffusive flux J_m decreases with time and tends towards a steady-state value while converging with the internalisation flux J_u. For the given set of parameter values in Fig. 3a, J_u increases steeply and reaches 97% of its steady-state value in less than 1 s (the maximum at $t \approx$30,000 s is not seen, of course), while J_m falls below 110% of J_m^{SS} after 31 s. A change in the radius has a dramatic impact on the fluxes, as can be seen when one compares panels a and b in Fig. 3, where the only difference is that r_0 has increased from 10 μm to 100 μm. The faster tendency of J_{u} towards J_m^{SS} for the case r_0=10 μm can be ascribed to the enhanced diffusion efficiency of the system with smaller radius acting at very short times.

3.2 Splitting the product $k\,K_H$

For a system with known D_M and r_0, knowledge of the steady-state flux J_m^{SS} allows the determination of the value of the product $k \cdot K_H$ from eqn. (15) but not the individual values of k and K_H. However, these individual values do affect the transient evolution of the flux J_m. Indeed, it is seen in Fig. 4 that keeping a fixed product for $k \cdot K_H = 2\times10^{-8}$ m s^{-1} (Slaveykova and Wilkinson 2002), the transient fluxes dramatically increase with the individual value of K_H increasing from 10^{-4} m to 0.1 m. Using a different set of parameters, Fig. 2 shows very different evolutions for $c_M(r_0,t)$ despite a common product $k\,K_H = 2\times10^{-3}$ m s^{-1}: the larger k, the faster the concentration approaches the steady-state value. For a fixed steady-state concentration at the active surface c_M^{SS}, the following physical picture for the parameters influencing the evolution of $c_M(r_0,t)$ can be suggested (Holub and Koryta 1965;Bates et al. 1982): adsorption is the predominant process at short t, but decays with increasing time; the rate of internalisation is less relevant at short times, but becomes significant from an intermediate stage on.

As a result, one concludes that the individual values of k and K_H can thus be found from the fitting of the transient behaviour of fluxes. For instance, it can also be seen that if J_u values are available at very short times, the slope of the tangent at the origin of the curve J_u vs. $\sqrt{t}$ provides $2kc_M^*\sqrt{D_M/\pi}$.

3.3.- How long does it take to reach steady state?

As discussed in section 3.1, the smaller the radius the sooner quasi-steady-state is reached. This fact supports the general suitability of the usual analysis of experimental data within the steady-state interpretative framework for small cells. However, the

approach to steady state can be quite slow for some combinations of the parameters (see Fig. 3b) and this might lead to significant errors in the determination of the characteristic parameters of the system if an inappropriate transient value is incorrectly taken as the final steady-state value. For instance, after 600 s, the concentration at the surface for curve k=10^{-4} s^{-1} in Fig 2 is still some 7% of the steady-state concentration value. Furthermore, in Fig. 3b the transient flux at t=72 s is still twice the true steady-state value; this would lead to 100% error in the determination of the product $k\,K_H$.

The availability of analytical expressions for the transient diffusive flux J_m allows the computation of the time necessary for a given required proximity to the steady state (Zoski et al. 1990). In order to enable a fast check of this time and to obtain more insight into the problem, we have constructed in Fig. 5 a contour plot for the particular case of J_m differing by 10% from J_m^{SS}. The plot can be used for any set of parameters following the model, because it can be demonstrated that three suitable dimensionless variables suffice to describe the model (Holub 1966). We have selected the following dimensionless parameters: $D_M t / r_0^2$ (which could be called a dimensionless time), K_H / r_0 (a dimensionless adsorption parameter) and $k\,r_0^2 / D_M$ (a dimensionless kinetic parameter). The logarithms of the dimensionless adsorption and kinetic parameters have been used as co-ordinates in Fig. 5. Each curve connects systems sharing the same dimensionless time to reach the condition J_m=1.1 J_m^{SS}.

Let us illustrate how Fig. 5 could be used with the particular D_M and r_0 data of Fig.3a: as the logarithms of the dimensionless parameters K_H / r_0 and $k\,r_0^2 / D_M$ in Fig. 3a are 0.30 and –5.30 respectively, we can read from Fig. 5 that log($D_M t / r_0^2$) is about 2.5 (the

point is in between the iso-lines labelled 2 and 3). This implies that approximately 30 s are needed to reach the prescribed proximity to steady state. If the individual values k and K_H were not known, but just their product (say 10^{-9} m·s^{-1}), we would have had not just a point in the diagram but the line $\log\left(\frac{K_H}{r_0}\right)+\log\left(\frac{k\,r_0^2}{D_M}\right)=-5$, which crosses contour curves with increasing values of the dimensionless times if the individual value of K_H is increased.

Observation of Fig. 5 suggests that, in general, increasing K_H delays the achievement of the steady state. This can be physically understood as larger K_H values imply larger amounts of M that must be transported towards the micro-organism surface, taking longer time. The pattern of the isocurves suggests two regions: the lower left region of relatively weak adsorption and slow kinetics, and the upper right region of relatively strong adsorption and fast kinetics. These two regions are separated by the main diagonal (defined by $kK_H = D_M / r_0$), thus indicating the critical role played by the product $k\,K_H$.

In the region above the diagonal ($kK_H r_0 / D_M >> 1$), the dimensionless time barely changes from a limiting value $D_M t / r_0^2 = 100/\pi$. In fact, this value can also be derived by realising that, due to the large k and K_H values, (spherical) diffusion becomes flux-limiting which comes to $\frac{1}{\sqrt{\pi D t}}+\frac{1}{r_0}=\frac{1.1}{r_0}$ (Bard and Faulkner 1980). Even at large K_H, the amount of matter adsorbed in this "flat" region is not large because the large internalisation rate considerably reduces the c_M^{SS}-value.

Under the diagonal ($kK_{\mathrm{H}}r_0 / D_{\mathrm{M}} << 1$) in Fig. 5, it can be seen that almost straight isocurves with slope 1 (fixed quotient of dimensionless adsorption and kinetic parameters) appear. Thus, moving within this region along a line with slope –1 (e.g. parallel to the diagonal corresponding to a fixed known product $k\,K_{\mathrm{H}}$) from left to right increases the dimensionless time to approach steady state. This can be physically understood because of the large amount of M required by the high Γ_{M} ($K_{\mathrm{H}}\ c_{\mathrm{M}}^{\mathrm{SS}}$ with a large value of K_{H} and $c_{\mathrm{M}}^{\mathrm{SS}} \approx c_{\mathrm{M}}^{*}$) under conditions of a the low value of $k\,K_{\mathrm{H}}$ (high K_{H} and very small k).

In conclusion, if the parameters of the system correspond to the region above the diagonal in Fig. 5, the standard estimation of the time to reach steady state based on just diffusion (i.e. $t \approx r_0^2 / D_{\mathrm{M}}$) is reasonable, but much larger times (dependent on the importance of adsorption and internalisation as well as on diffusion) are required when the parameters correspond to the right hand region below the diagonal.

3.4 The instantaneous steady-state approximation (ISSA).

Fig. 6a, which is similar to experimental figures in Hudson and Morel (1990); Knauer et al. (1997); Phinney and Bruland (1997); Fortin and Campbell (2000); Vasconcelos and Leal (2001); Slaveykova and Wilkinson (2002), shows Φ_m and Γ_{M} corresponding to fluxes depicted in Fig. 3a. We notice that, for these parameters, $\Phi_u = \Phi_m - \Gamma_{\mathrm{M}} << \Gamma_{\mathrm{M}}$ for quite a long time. After the building up of Γ_{M} in some 30 seconds, the system practically reaches a steady-state regime, reflected in the linear nature of the Φ_m and Φ_u for longer times. This linearity suggests one procedure to find the individual values of the parameters in the product $k\,K_{\mathrm{H}}$, if experimental access to very short times is not

feasible and it is not possible to distinguish between adsorbed and internalised amounts. Let us simplify the general model to just an instantaneous initial building of the surface concentration Γ_{M} up to the steady-state value, followed immediately by the steady-state regime flux:

$$\Phi_m(t) \approx K_{\mathrm{H}} c_{\mathrm{M}}^{\mathrm{SS}} + J_m^{\mathrm{SS}} t \qquad (24)$$

We refer to this simplified model as the instantaneous steady-state approximation (ISSA), as a way of rendering explicit the physical basis of transient fluxes underlying the usual interpretation of steady-state accumulated amounts (Slaveykova and Wilkinson 2002).

As expected, the dotted-dashed line in Fig. 6a representing equation (24) asymptotically tends to Φ_m for not too small *t*. In the case of Fig. 6a, the instantaneous steady-state approximation expressed in eqn. (24) is quite reasonable, due to the fast completion of the adsorption process. Thus, Φ_m-values for not too short times could be fitted to a straight line, the slope of which would yield J_m^{SS} and the intercept would yield $\Gamma_{\mathrm{M}}^{\mathrm{SS}} = K_{\mathrm{H}} c_{\mathrm{M}}^{\mathrm{SS}} = J_m^{\mathrm{SS}} / k$ from which *k* (and K_{H}) can be isolated.

As expected, if the system is still far from steady state, the method will yield erroneous values for K_{H}. With another set of parameters (with a lower D_{M} which for instance could apply to the diffusion of macromolecules), the plot of the cumulated fluxes (see Fig. 6b) clearly shows that the intercept is not a measure of Γ_{M} at steady state. From the slope of straight line fitting the rightmost part of Φ_m in Fig. 6b (the dotted-dashed line passing through points corresponding to *t*=300 s and *t*=600 s), a physically meaningless (negative) value of the product $K_{\mathrm{H}}\, k$ would be recovered and the intercept would predict

$K_{\mathrm{H}}c_{\mathrm{M}}^{\mathrm{SS}}$ around 35–fold the true value. The plot of the initial (t<600 s) fluxes for the system (see Fig. 7) highlights again that an apparent constancy of the flux can mask an extremely sluggish tendency towards steady state and also shows that after the concentration maximum the uptake flux is larger than the diffusional supply flux.

3.5 Application to experimental data

Slaveykova and Wilkinson (2002) reported values of the uptake of Pb^{2+} by *Chlorella vulgaris* under perfectly controlled conditions. In their figure 2, they plotted the amounts of Pb taken up by the cells in the categories of extractable and non-extractable with EDTA. By adding the two quantities, we obtain the experimental Φ_m as function of time, see diamond markers in Fig 8. The instantaneous steady-state approximation prescribes the linear regression of these points. Interpretation of the resulting intercept and slope according to eqn. (24) yields $J_m^{\mathrm{SS}}=4.79\times10^{-12}$ mol m^{-2} s^{-1} and $\Gamma_{\mathrm{M}}^{\mathrm{SS}} = K_{\mathrm{H}}c_{\mathrm{M}}^{\mathrm{SS}} = 1.89\times10^{-7}\,\mathrm{mol\,m^{-2}}$ respectively. Using eqns. (14) and (15) with c_{M}^{*} = 2.5×10^{-4} mol m^{-3}, $D_{\mathrm{M}}=9.45\times10^{-10}$ m^2s^{-1} and $r_0=1.8\times10^{-6}$ m, one finds $K_{\mathrm{H}}=7.55\times10^{-4}$ m and $k=2.54\times10^{-5}$ s^{-1}.

We show now that these recovered parameters agree with the analysis performed by Slaveykova and Wilkinson on the basis of two types of adsorption sites: one with physiological activity (where internalisation follows) and the other type without any further internalisation. As detailed in section 1.2, for low concentrations of M, the two-types-of-sites treatment reverts to the lineal one with k and K_{H} being averages of the two-types-of-sites parameters. The values of their reported parameters in our nomenclature and units are: $k_1=4.3\times10^{-4}$ s^{-1}; $K_{\mathrm{M},1} = 3.16\times10^{-3}\,\mathrm{mol\,m^{-3}}$; $\Gamma_{\mathrm{max},1} = 1.5\times10^{-7}$

mol m^{-2} ; $K_{M,2}$ = 8.9×10^{-3} mol m^{-3} and $\Gamma_{max,2}$ = 6.6×10^{-6} mol m^{-2} . Replacing their parameters in eqn. (13) one obtains that the expected *k*-value is 2.59×10^{-5} s^{-1} which compares favourably with our $k=2.54\times10^{-5}$ s^{-1}. Analogously, applying eqn. (12), the expected value of K_H from their parameters is 7.88×10^{-4} m which agrees with our value $K_H = 7.55\times10^{-4}$ m.

As seen in Fig 8, the parameters computed with ISSA also allow the computed Φ_m (with eqn. (23)) to fit very well the experimental data. The maximum in Γ_M cannot be seen because it appears at around 1000 minutes and the difference with the steady-state value is totally negligible. The time needed to reach 10% above the steady-state value J_m^{SS} can be read from Fig 5: the coordinates of the system with the recovered parameters are (2.61,-7.08) and have been marked with a cross, where an approximate non-dimensional time $10^{4.2}$ can be estimated (corresponding to $t\approx54$ s).

So the transient model proposed here explains the large measured accumulated amounts (when steady state is already settled) as due to an initial fast rise of Φ_m associated with adsorption. It is worth noticing that, although the transient fluxes–which are expected to be practically over in 54 seconds in this case- cannot be experimentally recorded, their consequences in the accumulated amount are significant.

CONCLUSIONS

The knowledge of analytical expressions for concentrations at the surface, fluxes and accumulated amounts along the evolution of the uptake allows to: i) support the general validity of the analyses of the fluxes within the steady state framework (i.e. determining

a fixed product $k\ K_H$); ii) caution that for some combination of the parameters (low D_M and k values; large r_0 and K_H values) significant loss of precision could arise from such an analysis due to longer transient regimes; iii) check any suggested splitting of the product $k\ K_H$ if accumulated amounts are known; iv) the individual determination of k and K_H if transient data are available; iv) validate the ISSA method (where K_H is determined from the linear regression associated to eqn. (24)). Implementation of the ISSA method with experimental data from the literature is satisfactory.

Acknowledgements

The authors gratefully acknowledge support of this research by the Spanish Ministry of Education and Science (DGICYT: Project BQU2000-0642), by the European Community under contract EVK1-CT2001-86 and from the "Comissionat d'Universitats i Recerca de la Generalitat de Catalunya". An Iberdrola professorship to HvL is also acknowledged.

List of symbols:

Symbol	**Name**	**Units**	**Equation**
c_M	concentration of the species M being taken up	mol m^{-3}	(1)
c_M^*	bulk concentration of the species M being taken up	mol m^{-3}	(4)
c_M^{SS}	steady state concentration at the surface ($r=r_0$)	mol m^{-3}	(14)

D_M	diffusion coefficient of species M	m^2s^{-1}	(1)
F	experfc function	-	(20)
J_m	diffusive flux	mol m^{-2} s^{-1}	(6)
J_u	uptake flux	mol m^{-2} s^{-1}	(7)
J_m^{SS}	steady state diffusive flux	mol m^{-2} s^{-1}	(15)
J_m^*	diffusion-limited steady-state flux	mol m^{-2} s^{-1}	(16)
K_H	linear adsorption coefficient	m	(2),(3)
$K_{M,1}$, $K_{M,2}$	half saturation constants	mol m^{-3}	
k	internalisation kinetic constant	s^{-1}	(3)
k_1	internalisation kinetic constant for physiologically active site	s^{-1}	(11)
r	radial ordinate	m	(1)
r_0	radius of organism	m	Fig 1
t	time	s	(1)
α, β	auxiliary parameters	$s^{-1/2}$	(17), (18)
Γ_M	surface concentration (in the linear model)	mol m^{-2}	(2),(3)
Γ_1, Γ_2	surface concentrations (in the Langmuirian model)	mol m^{-2}	(10)
Φ_u	cumulative uptake	mol m^{-2}	(8)

References

Abramowitz, M., Stegun, I. A., 1986, *Handbook of Mathematical Functions*, Dover, New York.

Bard, A. J., Faulkner, L. R., 1980, *Electrochemical Methods, Fundamentals and Applications*, Wiley, New York.

Bates, S. S., Tessier, A., Campbell, P. G. C., Buffle, J., 1982. Zinc adsorption and transport by *Chlamydomonas-variabilis* and *Scenedesmus-subspicatus* (*Chlorophyceae*) grown in semi- continuous culture. *J.Phycol.* 18, 521-529.

Campbell, P. G. C. 1995, Interactions between Trace Metal and Aquatic Organisms: A Critique of the Free-ion Activity Model, in Tessier, A., Turner, D. R. (Eds), *Metal Speciation and Bioavailability in Aquatic Systems*, John Wiley & Sons, Chichester, pp. 45-102.

Campbell, P. G. C., Errecalde, O., Fortin, C., Hiriart-Baer, W. R., Vigneault, B., 2002. Metal bioavailability to phytoplankton - applicability of the biotic ligand model. *Comp.Biochem.Physiol.C* 133, 189-206.

Croot, P. L., Karlson, B., Van Elteren, J. T., Kroon, J. J., 1999. Uptake of ^{64}Cu oxine by marine phytoplankton. *Environ.Sci.Technol.* 33, 3615-3621.

DeJong, H. G., van Leeuwen, H. P., 1987. Voltammetry of Metal-Complex Systems with Different Diffusion- Coefficients of the Species Involved .2. Behavior of the Limiting Current and Its Dependence on Association Dissociation Kinetics and Lability. *J.Electroanal.Chem.* 234, 17-29.

Fortin, C., Campbell, P. G. C., 2000. Silver uptake by the green alga Chlamydomonas reinhardtii in relation to chemical speciation: Influence of chloride. *Environ.Toxicol.Chem.* 19, 2769-2778.

Fortin, C., Campbell, P. G. C., 2001. Thiosulfate enhances silver uptake by a green alga: Role of anion transporters in metal uptake. *Environ.Sci.Technol.* 35, 2214-2218.

Hassler, C. S., Wilkinson, K. J., 2003. Failure of the biotic ligand and free-ion activity models to explain zinc bioaccumulation by Chlorella kesslerii. *Environ.Toxicol.Chem.* 22, 620-626.

Heyrovsky, J., Kuta, J., 1966, *Principles of Polarography*, Academic Press, New York.

Holub, K., 1966. Surface reaction of an adsorbed substance transported by diffusion to a spherical electrode. *Collect.Czech.Chem.Commun.* 31, 1655-1665.

Holub, K., Koryta, J., 1965. Surface reaction of adsorbed substance transported by diffusion to a plane electrode. *Collect.Czech.Chem.Commun.* 30, 3785-3796.

Holub, K., van Leeuwen, H. P., 1984. Influence of reactant adsorption on limiting currents in normal pulse polarography .2. Theory for the stationary, spherical electrode. *J.Electroanal.Chem.* 162, 55-65.

Hudson, R. J. M., 1998. Which aqueous species control the rates of trace metal uptake by aquatic biota? Observations and predictions of non- equilibrium effects. *Sci.Total Envir.* 219, 95-115.

Hudson, R. J. M., Morel, F. M. M., 1990. Iron transport in marine-phytoplankton - kinetics of cellular and medium coordination reactions. *Limnol.Oceanogr.* 35, 1002-1020.

Hudson, R. J. M., Morel, F. M. M., 1993. Trace-metal transport by marine microorganisms - implications of metal coordination kinetics. *Deep-Sea.Res.Part I* 40, 129-150.

KarpBoss, L., Boss, E., Jumars, P. A., 1996. Nutrient fluxes to planktonic osmotrophs in the presence of fluid motion. *Oceanogr.Mar.Biol.* 34, 71-107.

Knauer, K., Behra, R., Sigg, L., 1997. Adsorption and uptake of copper by the green alga Scenedesmus subspicatus (Chlorophyta). *J.Phycol.* 33, 596-601.

Kujawinski, E. B., Farrington, J. W., Moffett, J. W., 2000. Importance of passive diffusion in the uptake of polychlorinated biphenyls by phagotrophic protozoa. *Appl.Environ.Microbiol.* 66, 1987-1993.

Kuma, K., Tanaka, J., Matsunaga, K., Matsunaga, K., 2000. Effect of hydroxamate ferrisiderophore complex (ferrichrome) on iron uptake and growth of a coastal marine diatom, Chaetoceros sociale. *Limnol.Oceanogr.* 45, 1235-1244.

Lazier, J. R. N., Mann, K. H., 1989. Turbulence and the diffusive layers around small organisms. *Deep-Sea.Res.* 36, 1721-1733.

Mirimanoff, N., Wilkinson, K. J., 2000. Regulation of Zn accumulation by a freshwater gram-positive bacterium (Rhodococcus opacus). *Environ.Sci.Technol.* 34, 616-622.

Morel, F. M. M., Hering, J. G. 1993, Complexation, *Principles and Applications of Aquatic Chemistry*, vol. 197 John Wiley, New York, pp. 319-420.

Oldham, K. B., Myland, J. C. 1994, Steady-state voltammetry, *Fundamentals of Electrochemical Science*, Academic Press, San Diego, pp. 263-308.

Phinney, J. T., Bruland, K. W., 1997. Trace metal exchange in solution by the fungicides Ziram and Maneb (dithiocarbamates) and subsequent uptake of lipophilic organic zinc, copper and lead complexes into phytoplankton cells. *Environ.Toxicol.Chem.* 16, 2046-2053.

Pinheiro, J. P., van Leeuwen, H. P., 2001. Metal speciation dynamics and bioavailability. 2. Radial diffusion effects in the microorganism range. *Environ.Sci.Technol.* 35, 894-900.

Sanford, L. P., Crawford, S. M., 2000. Mass transfer versus kinetic control of uptake across solid- water boundaries. *Limnol.Oceanogr.* 45, 1180-1186.

Slaveykova, V. I., Wilkinson, K. J., 2002. Physicochemical aspects of lead bioaccumulation by Chlorella vulgaris. *Environ.Sci.Technol.* 36, 969-975.

Stumm, W., Morgan, J. J. 1996, Trace metals: cycling, regulation, and biological role, *Aquatic Chemistry*, 3rd edn, John Wiley, New York, pp. 614-671.

Sunda, W. G., Huntsman, S. A., 1998. Control of Cd concentrations in a coastal diatom by interactions among free ionic Cd, Zn, and Mn in seawater. *Environ.Sci.Technol.* 32, 2961-2968.

Tessier, A., Buffle, J., Campbell, P. G. C. 1994, Uptake of Trace Metals by Aquatic Organisms, in Buffle, J., DeVitre, R. R. (Eds), *Chemical and Biological Regulation of Aquatic Systems*, Lewis Publishers, Boca Raton, FL, pp. 197-230.

van Leeuwen, H. P., Pinheiro, J. P., 2001. Speciation dynamics and bioavailability of metals. Exploration of the case of two uptake routes. *Pure Appl.Chem.* 73, 39-44.

Vasconcelos, M. T. S. D., Leal, M. F. C., 2001. Adsorption and uptake of Cu by Emiliania huxleyi in natural seawater. *Environ.Sci.Technol.* 35, 508-515.

Whitfield, M., Turner, D. R. 1979, Critical assessment of the relationship between biological thermodynamic and electrochemical availability, in Jenne, E. A. (Ed.), *Chemical Modeling in Aqueous Systems*, American Chemical Society, Washington DC, pp. 657-680.

Wolf-Gladrow, D. A., Bijma, J., Zeebe, R. E., 1999. Model simulation of the carbonate chemistry in the microenvironment of symbiont bearing foraminifera. *Mar.Chem.* 64, 181-198.

Zoski, C. G., Bond, A. M., Allinson, E. T., Oldham, K. B., 1990. How long does it take a microelectrode to reach a voltammetric steady-state? *Anal.Chem.* 62, 37-45.

Figure Captions:

FIG. 1: Outline of the uptake model showing the spherical diffusion of species M through the medium. Linear adsorption onto the surface is followed by first order internalisation kinetics.

FIG. 2: Evolution of $c_{\mathrm{M}}(r_0,t)/c_{\mathrm{M}}^{*}$ for five combinations of K_{H} and k yielding a common product 2×10^{-3} m s^{-1} (estimated from (Hassler and Wilkinson 2003)). Curves for k = 1 s^{-1}, k = 10^{-1} s^{-1}, k = 2×10^{-2} s^{-1} , k =10^{-3} s^{-1} and k =10^{-4} s^{-1} converge towards $c_{\mathrm{M}}^{\mathrm{SS}}/c_{\mathrm{M}}^{*}$ = 0.005 (dashed horizontal line). The grey area corresponds to a range of some reported values of k (Hudson and Morel 1990;Hudson and Morel 1993). Other parameters: D_{M}=10^{-9} m^2 s^{-1} and r_0 =0.1 mm.

FIG. 3 Fluxes vs. t. Upper solid curve: diffusive flux J_m. Lower dotted curve: internalisation flux J_{u}. Parameters: K_{H}=$2\cdot10^{-5}$m, k=$5\cdot10^{-5}$ s^{-1}, D_{M}=10^{-9} m^2 s^{-1} and c_{M}^{*} =10^{-3} mol ·m^{-3}**.** a): Case r_0=10 μm. b): Slow approach of J_m towards steady state (horizontal dashed line, J_m^{SS} eqn. (15)) for r_0=0.1 mm.

FIG. 4 Transient fluxes for four different combinations of K_{H} and k yielding a common product 2×10^{-8} m s^{-1}. Lines with K_{H}=0.1 m, K_{H}=10^{-2} m, K_{H}=10^{-3} m and K_{H}=10^{-4} m converge towards J_m^{SS} = 2×10^{-11} mol·m^{-2}·s^{-1}. The grey area corresponds to a range of some reported values of K_{H} (Slaveykova and Wilkinson 2002;Hassler and Wilkinson 2003). Other parameters as in Fig. 3a.

FIG. 5: Contour plot of the dimensionless time $\left(D_{\mathrm{M}}t/r_0^2\right)$ needed for J_m to reach 1.1 J_m^{SS} in terms of the logarithm of the dimensionless adsorption parameter $\left(K_{\mathrm{H}}/r_0\right)$, in abscissas (bottom axis), and the logarithm of the dimensionless internalisation parameter $\left(k\,r_0^2/D_{\mathrm{M}}\right)$, in ordinates (left axis). The number on each curve indicates the value of $\log\left(D_{\mathrm{M}}t/r_0^2\right)$. The diagonal (dashed line) corresponds to $kK_{\mathrm{H}}r_0 = D_{\mathrm{M}}$. The point marked with a cross corresponds to the parameter values recovered from experimental data described in section 3.5. The outer (up and right) axes correspond to the case r_0=10 μm, D_{M}=10^{-10} $\mathrm{m^{-2}s^{-1}}$, so that the labels of the isocurves can be directly read for this particular case as log(*t*) without any dimensionless variable.

FIG. 6: Evolution of total cumulative supply Φ_m (see eqn. (23)) and surface concentration $\Gamma_{\mathrm{M}}(t) = K_{\mathrm{H}}c_{\mathrm{M}}(r_0,t)$. The dashed line corresponds to the steady-state surface concentration $\Gamma_{\mathrm{M}}^{\mathrm{SS}} = K_{\mathrm{H}}c_{\mathrm{M}}^{\mathrm{SS}}$. a) With parameters as in Fig. 3a, an asymptotic behaviour of the dotted-dashed line $K_{\mathrm{H}}c_{\mathrm{M}}^{\mathrm{SS}} + J_m^{\mathrm{SS}}t$ (equation (24)) with respect to Φ_m can be seen. b): In a case with k= 10^{-1} $\mathrm{s^{-1}}$, K_{H}=10^{-4} m, D_{M}=10^{-11} $\mathrm{m^2\ s^{-1}}$, c_{M}^{*}=10^{-3} mol $\cdot\mathrm{m^{-3}}$ and r_0=0.01 cm, a linear fit (dotted-dashed line) of relatively long time values of Φ_m can lead to erroneous determinations of K_{H}.

FIG. 7: Plot of the fluxes with the same parameters as in Fig. 6b, showing that proximity to steady state can require relatively long times. Dotted line stands for J_u.

FIG. 8: Fitting of experimental data from Fig. 2 of ref. (Slaveykova and Wilkinson 2002) (markers ♦) with Φ_m given by eqn. (23) using parameters retrieved through the

linear regression associated to eqn. (24) : K_H=7.55×10^{-4} m and k=2.54×10^{-5} s^{-1} together with D_M=9.45×10^{-10} m^{2}s^{-1} and r_0=1.8×10^{-6} m. Theoretical Φ_u and Γ_M –curves are also included.

Published in Marine Chemistry 2004, vol 85, p 89-102

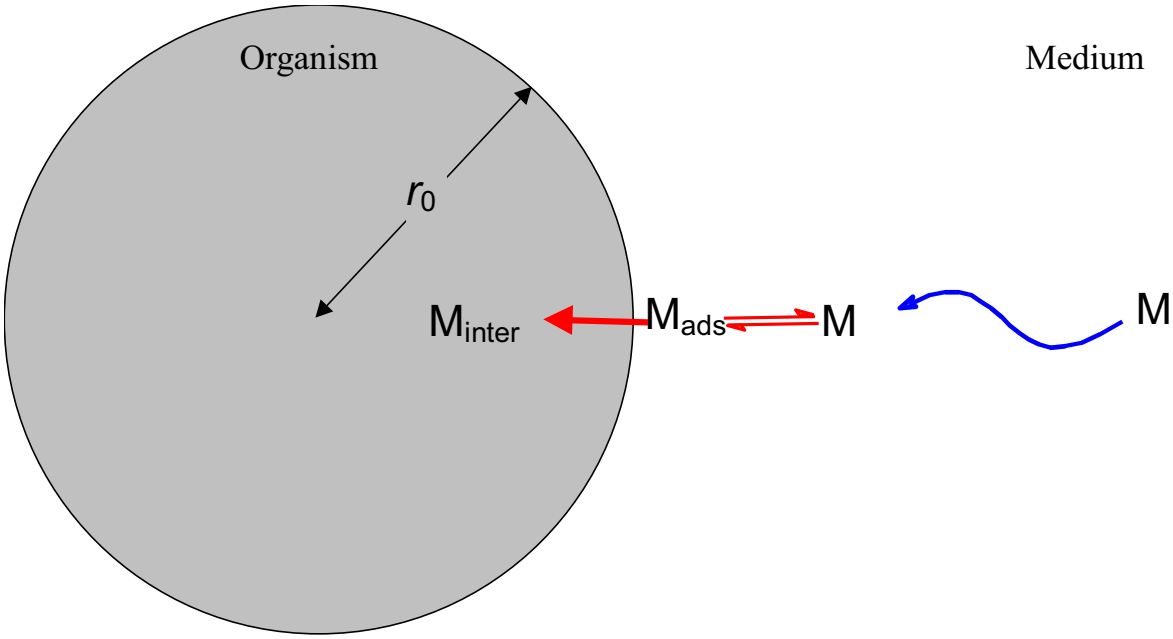

Fig 1

Published in Marine Chemistry 2004, vol 85, p 89-102

Fig 2

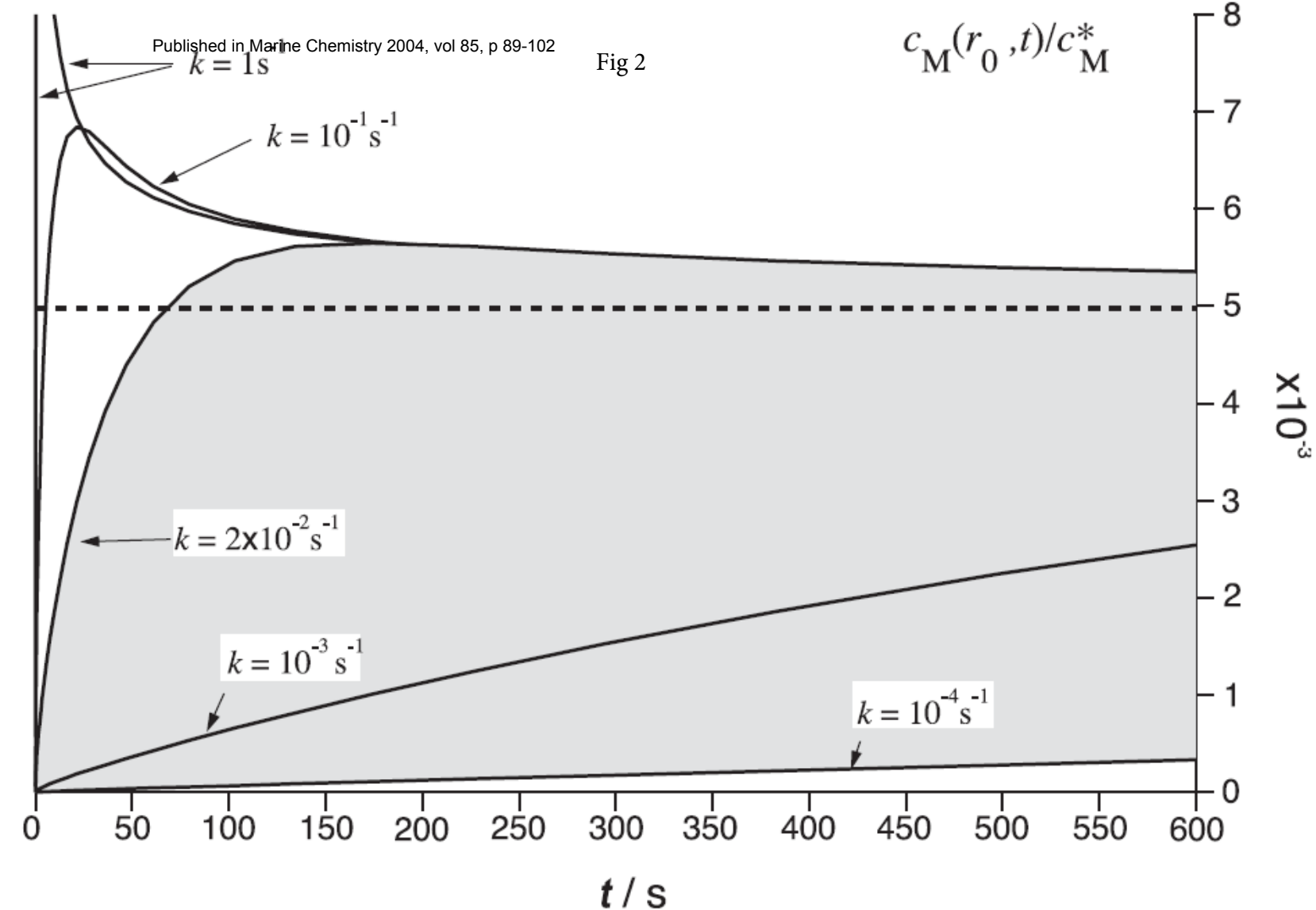

Published in Marine Chemistry 2004, vol 85, p 89-102

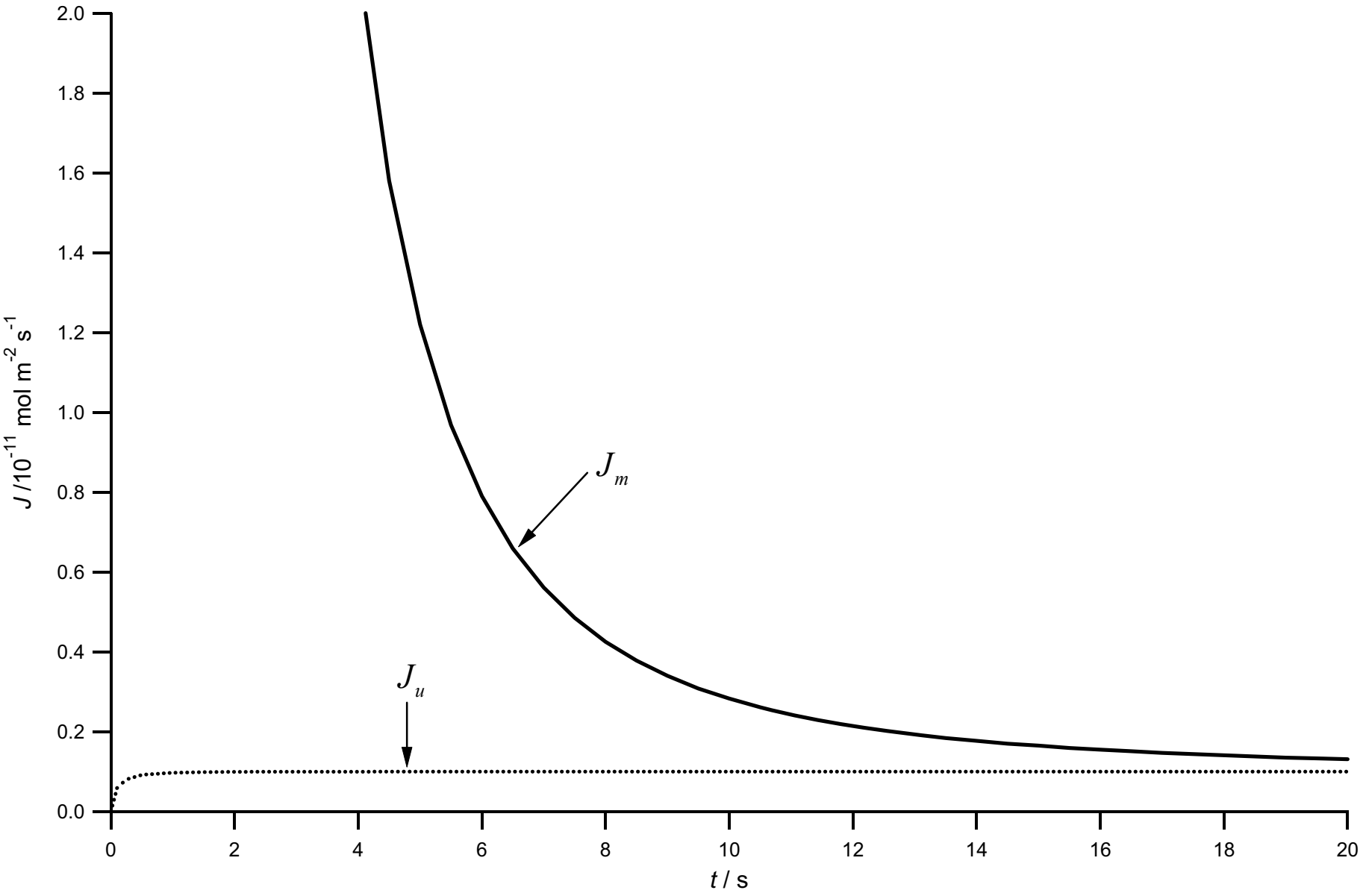

Fig 3a

Published in Marine Chemistry 2004, vol 85, p 89-102

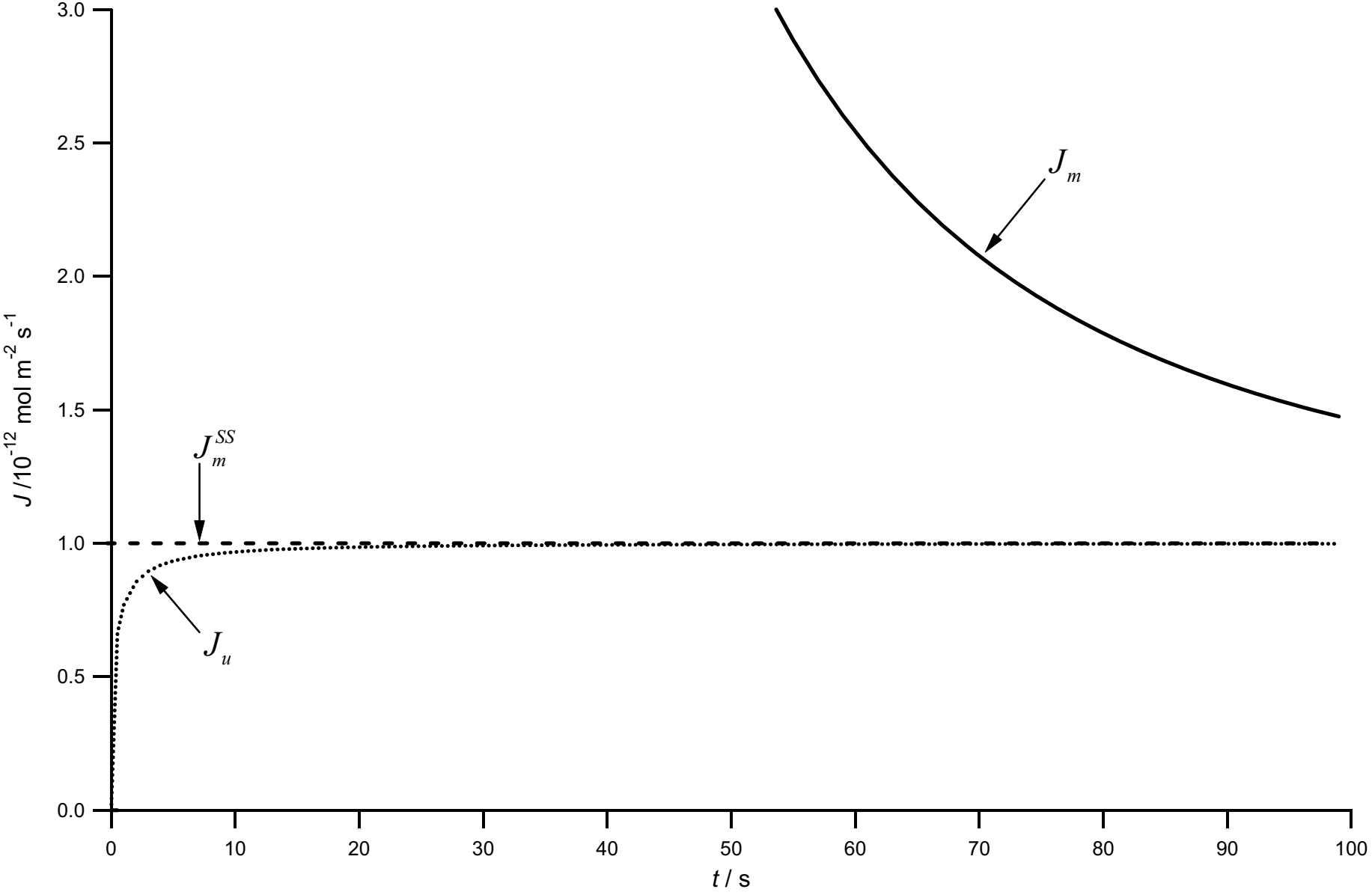

Fig 3b

Published in Marine Chemistry 2004, vol 85, p 89-102

Fig 4

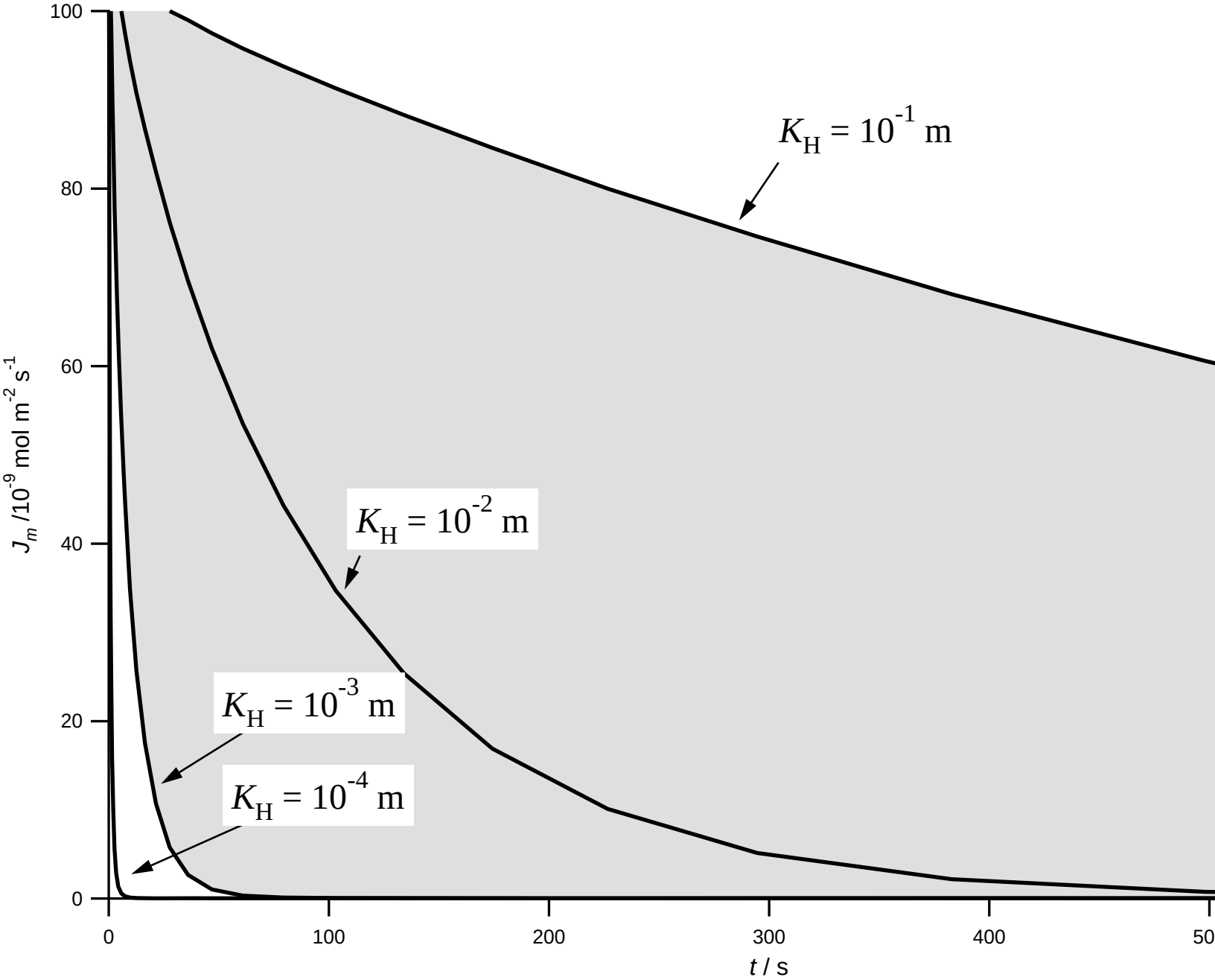

Published in Marine Chemistry 2004, vol 85, p 89-102
DOI: 10.1016/j.marchem.2003.09.005
reprints to galceran@quimica.udl.cat

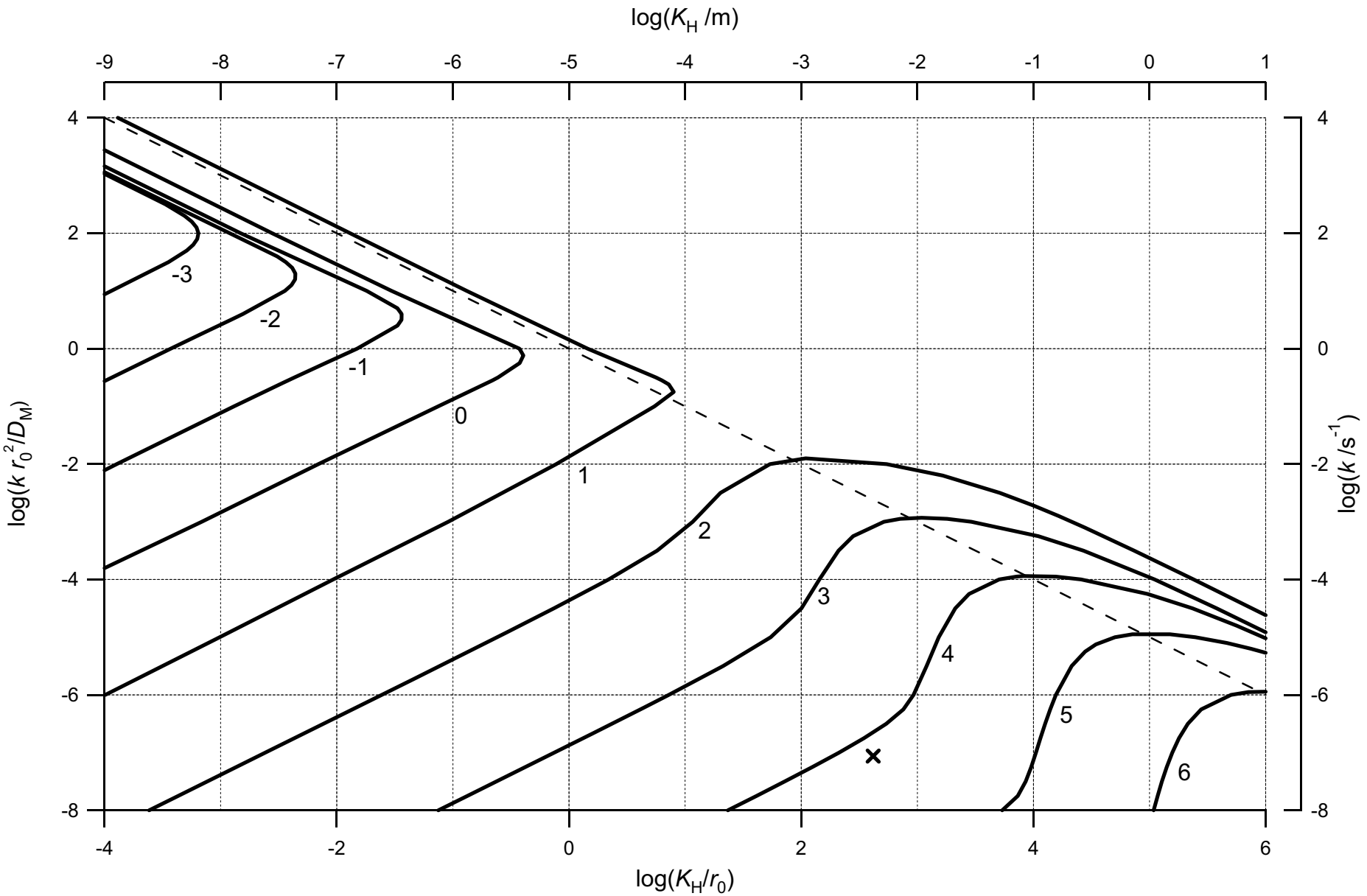

Fig 5

Published in Marine Chemistry 2004, vol 85, p 89-102
DOI: 10.1016/j.marchem.2003.09.005
reprints to galceran@quimica.udl.cat

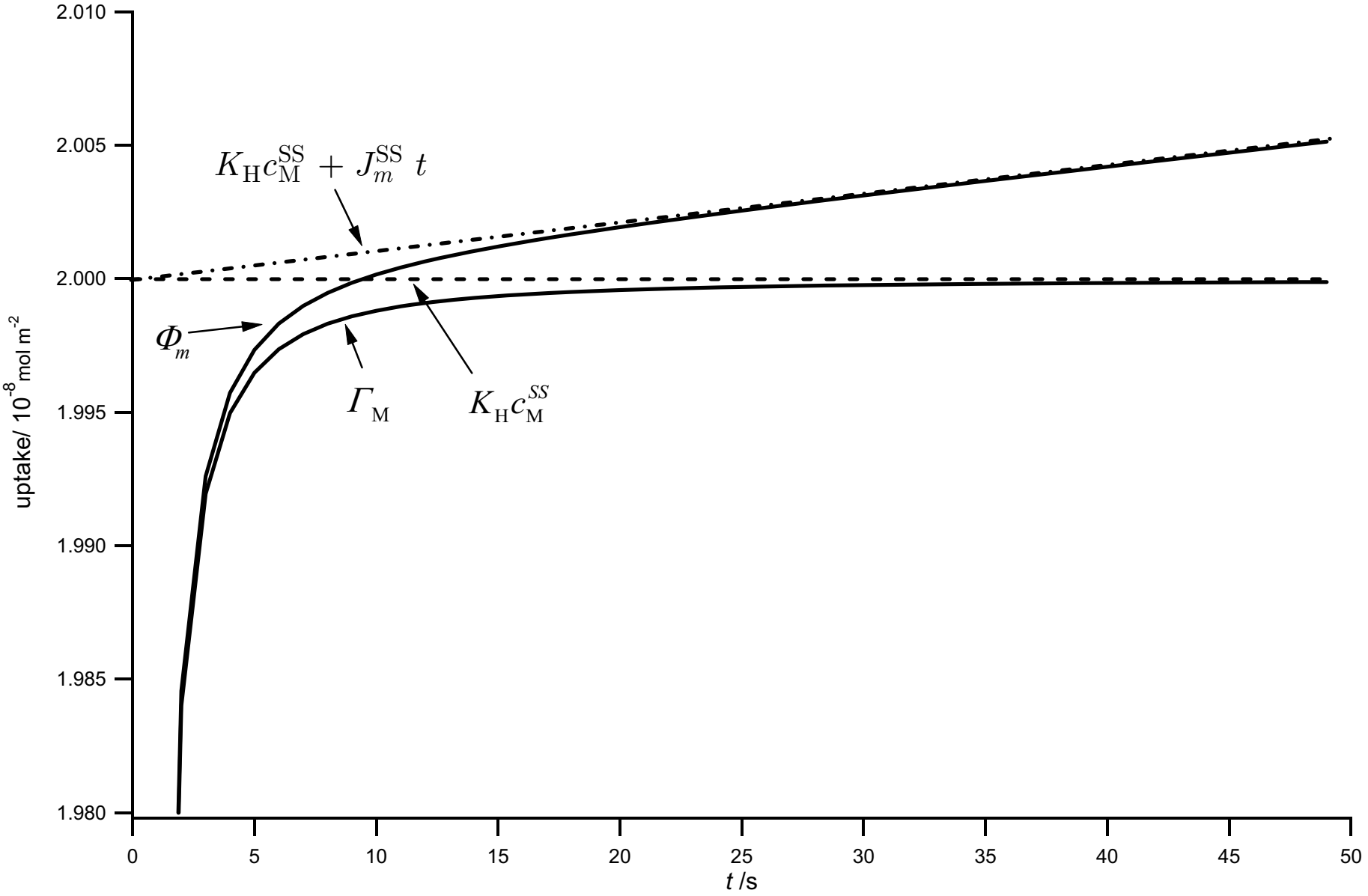

Fig 6a

Published in Marine Chemistry 2004, vol 85, p 89-102
DOI: 10.1016/j.marchem.2003.09.005

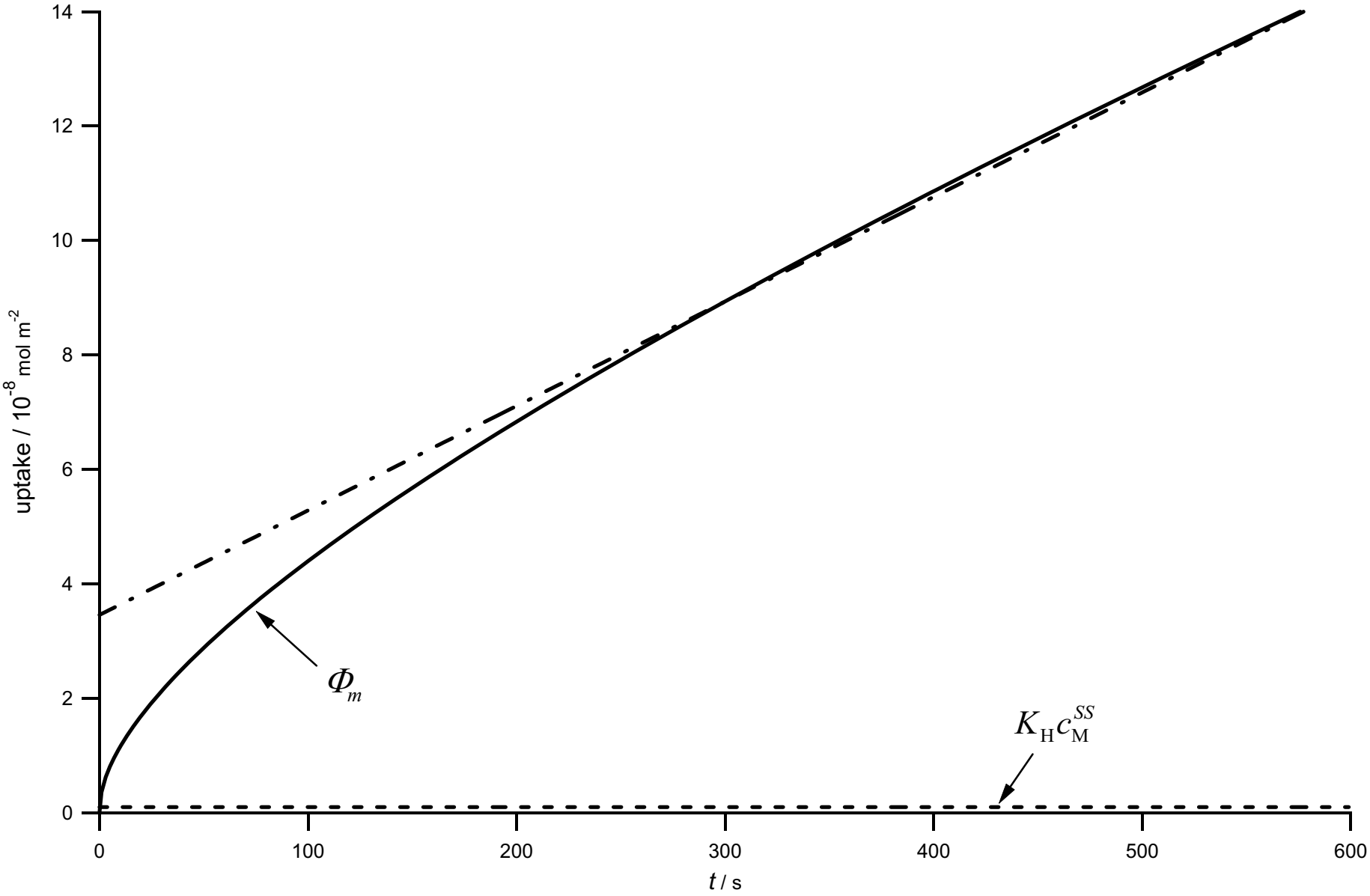

Fig 6b

Published in Marine Chemistry 2004, vol 85, p 89-102
DOI: 10.1016/j.marchem.2003.09.005

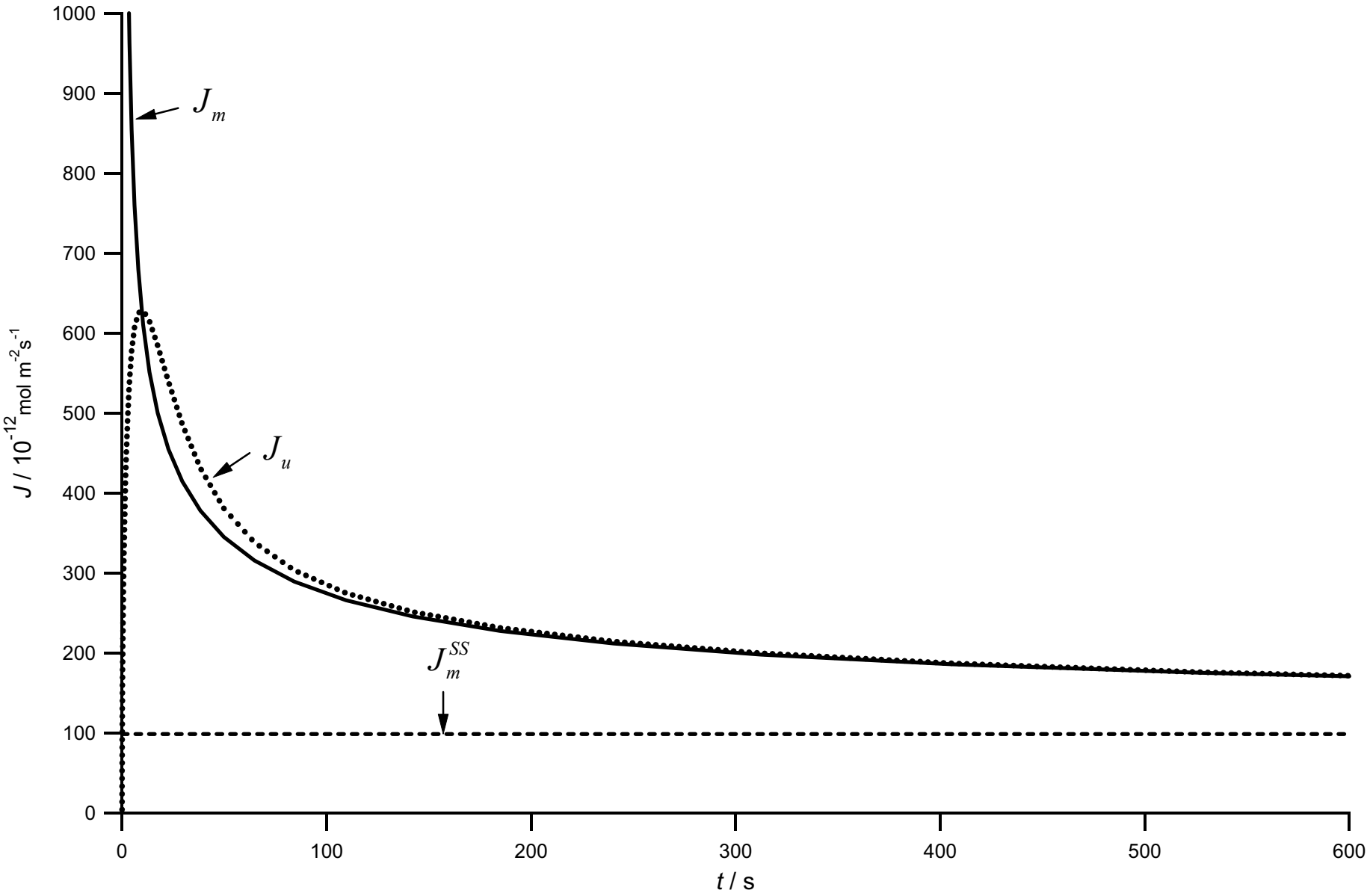

Fig 7

Published in Marine Chemistry 2004, vol 85, p 89-102
DOI: 10.1016/j.marchem.2003.09.005
reprints to galceran@quimica.udl.cat

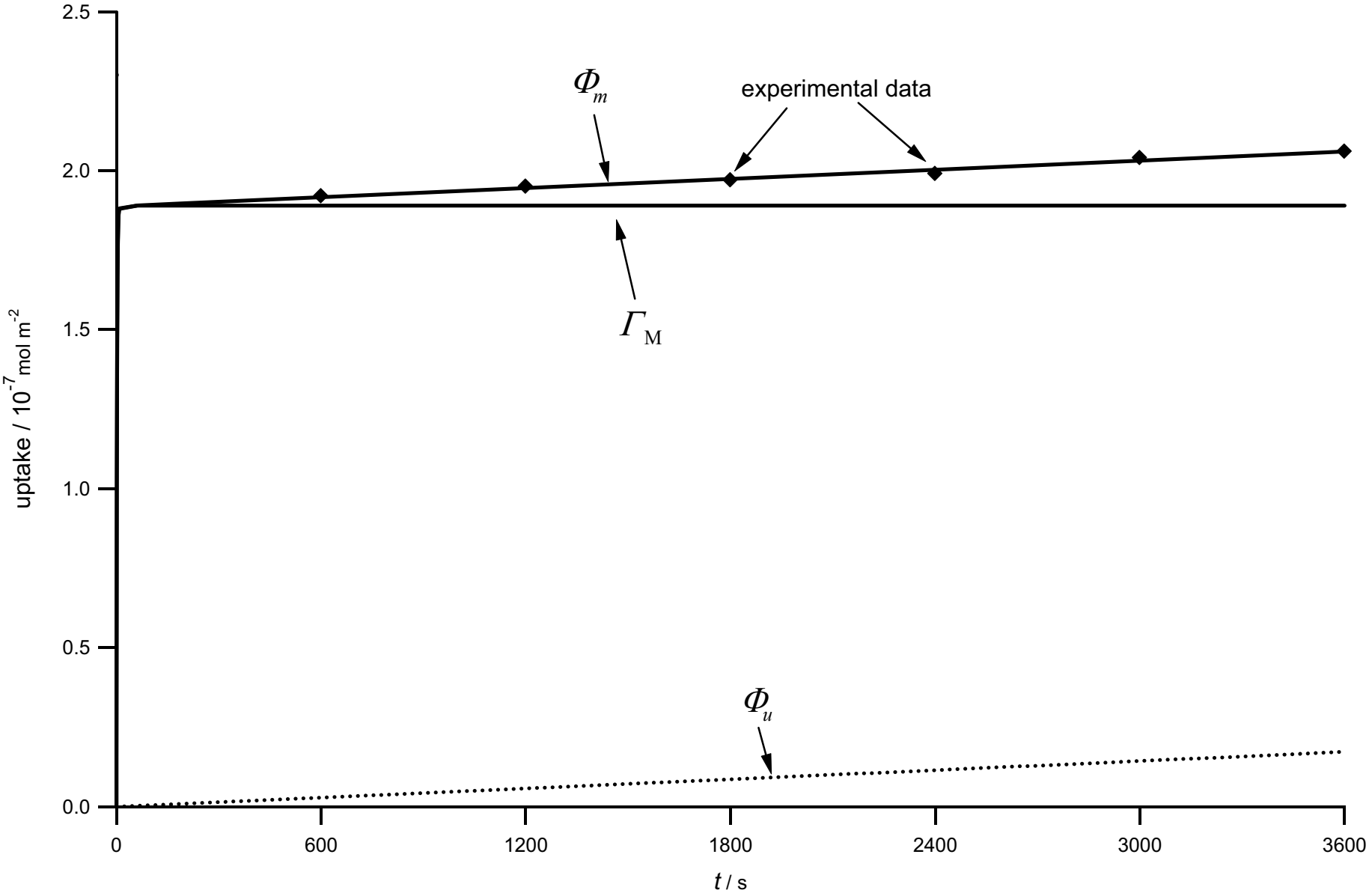

Fig 8